

DANG THY MYLINH<sup>\*,\*\*</sup>, DAE-HO YOON<sup>\*\*</sup>, CHANG-YEOUL KIM<sup>\*,#</sup>**ALUMINUM NITRIDE FORMATION FROM ALUMINUM OXIDE/PHENOL RESIN SOLID-GEL MIXTURE BY CARBOTHERMAL REDUCTION NITRIDATION METHOD****WYTWARZANIE AZOTKU ALUMINIUM Z ŻELOWEJ MIESZANINY TLENKU ALUMINIUM Z ŻYWICĄ FENOLOWĄ METODĄ AZOTOWANIA PODCZAS CARBOTERMICZNEJ REDUKCJI**

Hexagonal and cubic crystalline aluminum nitride (AlN) particles were successfully synthesized using phenol resin and alpha aluminum oxide ( $\alpha$ -Al<sub>2</sub>O<sub>3</sub>) as precursors through new solid-gel mixture and carbothermal reduction nitridation (CRN) process with molar ratio of C/Al<sub>2</sub>O<sub>3</sub> = 3. The effect of reaction temperature on the decomposition of phenol resin and synthesis of hexagonal and cubic AlN were investigated and the reaction mechanism was also discussed. The results showed that  $\alpha$ -Al<sub>2</sub>O<sub>3</sub> powder in homogeneous solid-gel precursor was easily nitrated to yield AlN powder during the carbothermal reduction nitridation process. The reaction temperature needed for a complete conversion for the precursor was about 1700°C, which much lower than that when using  $\alpha$ -Al<sub>2</sub>O<sub>3</sub> and carbon black as starting materials. To our knowledge, phenol resin is the first time to be used for synthesizing AlN powder via carbothermal reduction and nitridation method, which would be an efficient, economical, cheap assistant reagent for large scale synthesis of AlN powder.

*Keywords:* aluminum nitride, powder, carbothermal reduction, nitridation, solid-gel mixture

**1. Introduction**

In recent years, thermal management of electronic parts such as CPU, semiconducting chips, and light emitting diode (LED) is key issue for their performance. In order to enhance the performance with the rapid heat dissipation rate from integrated circuits (IC) for which only ceramics dielectric substrate is essential and many researchers have widely studied materials with high thermal conductivity. Aluminum nitride (AlN) is an important member of the group III nitrides with superior thermal conductivity (320 W m<sup>-1</sup>·K<sup>-1</sup>). It is a promising advanced ceramic material with many excellent properties such as high band gap of around 6.2 eV, high electrical resistivity (10<sup>13</sup>), small dielectric constant (8.8 at 1 MHz), and low thermal expansion coefficient (which closely matched that of silicon, 4.7×10<sup>-6</sup> K<sup>-1</sup>) [1,2].

Many methods have been reported on the production of AlN powders including direct nitridation of Al metal in N<sub>2</sub> or NH<sub>3</sub> atmosphere, carbothermal reduction of Al<sub>2</sub>O<sub>3</sub> in Al<sub>2</sub>O<sub>3</sub>-C-N<sub>2</sub> system or Al<sub>2</sub>O<sub>3</sub>-NH<sub>3</sub>-C<sub>3</sub>H<sub>8</sub> system [3-5], vapor phase synthesis [6,7], plasma synthesis [8,9], and self-propagating high temperature synthesis [10,11]. Among them, two primary processes to manufacture AlN powders commercially are direct nitridation and carbothermal reduction [12]. Comparatively, AlN powders produced by carbothe-

mal reduction nitridation (CRN) have the advantages of better purity, sinterability, and stability against humidity. However, carbothermal reduction method has also disadvantages, such as the notorious difficulty to homogeneously mix the starting materials, the high cost based on the high reactions temperature and demand of high purity Al<sub>2</sub>O<sub>3</sub> and carbon black for the fabrication of high purity AlN powder. Several modified CRN methods were suggested to compensate for homogeneous mixing, for example, Silverman [13] synthesized AlN powders from colloidal aluminum oxide precursor dispersed in a polymer matrix and Hashimoto [14] also prepared AlN powders from aluminum polynuclear complexes and glucose. Their researches show that the homogeneous mixing of starting materials can affect reaction conditions and properties of AlN powders. Therefore, the selection of raw materials and a homogeneous mixture of precursor have become key factors of CRN method.

In this paper, AlN powders are synthesized from the mixture of aluminum oxide dispersed in phenol resin which is synthesized to produce homogeneous mixture of alumina and carbon powders as a precursor to AlN. To our knowledge, phenol resin is the first try to synthesize AlN powders with large scale. Moreover, AlN powders were consisted of wurtzite hexagonal and cubic AlN which had higher thermal conductivity. It is well known that the thermal conductivity of cubic AlN

\* NANO CONVERGENCE INTELLIGENCE MATERIAL TEAM, KOREA, INSTITUTE OF CERAMIC, ENGINEERING AND TECHNOLOGY SONO-RO 101, JINJU-SI, KYEONG-SANGNAM-DO, 660-031 KOREA

\*\* ELECTRONIC MATERIALS LAB., SCHOOL OF ADVANCED MATERIALS SCIENCE AND ENGINEERING, SUNGKYUNKWAN. UNIV. SUWON 440-746, REPUBLIC OF KOREA

# Corresponding author: cykim15@kicet.re.kr

(about  $250\text{--}600\text{ W m}^{-1}\cdot\text{K}^{-1}$ ) is larger than that of hexagonal AlN [15]. So, we think that the formation of cubic AlN will increase the thermal conductivity of the AlN sintered product or AlN/polymer composites.

## 2. Experimental procedure

The starting materials are  $\alpha\text{-Al}_2\text{O}_3$  powder, supplied by the Kodell Co., Ltd., Korea and phenol resin which was resol type diluted with 50% methanol solvent, supplied by the Kang Nam chemical Co., Ltd., Korea. 0.1 mole of alumina powders was added to 0.05 mole phenol resin and the solution, subsequently, was blended with magnetic stirrer to become totally homogeneous. Alumina was dispersed in liquid phase. The resultant solid gel mixture was dried at  $110^\circ\text{C}$  to remove solvent. As result, dark brown solid gel mixture was obtained and then ground into gel powder as a powder precursor. The thermogravimetric (TG) analyses (Fig. 2) indicated that the decomposition of 80% the phenol resin into carbon was completed below  $800^\circ\text{C}$ . As the solid-gel mixing proceeds,  $\text{Al}_2\text{O}_3$  particles uniformly dispersed into carbon matrix, which is formed by the dehydration and dehydrogenation of phenol resin.

The CRN reaction of the precursor was performed in graphite furnace. The samples were held in graphite crucible. Before heating, the furnace was vacuumed and then flushed with nitrogen gas to eliminate oxygen before the reaction. The precursor mixture was heated in a flowing nitrogen gas at various temperatures in the range of  $1300\text{--}1800^\circ\text{C}$  for 2h. The flow rate of nitrogen gas (99.999% in purity) was  $1\text{ L min}^{-1}$ . Thermogravimetry- differential thermal analysis (TG-DTA) was performed with thermoanalyzer from R.T. to  $1000^\circ\text{C}$  in  $\text{N}_2$  atmosphere and X-ray diffraction patterns (XRD) was collected on Rigaku X-ray diffractometer (XRD- 6000 diffractometer with  $\text{CuK}\alpha$  radiation). Field emission-scanning electron microscopy (FE-SEM, JSM-6700F, JEOL, Japan) was used to characterize the morphology of particles. Size distributions of AlN powders were measured by particle size analyzing (LPSA).

## 3. Results and discussion

Thermal degradation of phenol resin was investigated by many researchers. Resol type of phenol resin is bridged by methylene ( $-\text{CH}_2-$ ) and the formation of cresol, phenol and xylenol occurs, depending on the position of scission of formaldehyde-phenol resin [16], as shown in Fig. 1. Lin *et al* [17] observed the decrease of ( $=\text{CH}-$ ) bonds with temperature and the increase of diphenol ether. So, we observed five degradation states of aluminum oxide/phenol resin mixtures under  $600^\circ\text{C}$  as shown in Fig. 2. The first state of weight loss of about 0.4% in the range of  $20\text{--}150^\circ\text{C}$  (region I) could be attributed to the evaporation of moisture and trapped solvent (methanol) from precursor. The weight loss in range of  $150\text{--}250^\circ\text{C}$  (region II) is about 2.1% due to the decomposition of methylene bridge ( $-\text{CH}_2-$ ) to form cresol, phenol and xylenol via the scission of formaldehyde and phenol resin. Beyond  $250^\circ\text{C}$  the thermal decomposition of phenol resin begins to take place, and decomposition of ( $=\text{CH}-$ ) group from cresol and xylenol might

occur between  $250$  and  $400^\circ\text{C}$  (region III) [16]. The region IV in  $400\text{--}600^\circ\text{C}$ , 10% weight loss is believed to originate from the decomposition and carbonization of phenol resin, that is, the decomposition of ( $-\text{OH}$ ) and ( $=\text{CH}-$ ) group from phenol resin. In the region V between  $600$  and  $1300^\circ\text{C}$ , carbon was degraded gradually to reduce  $\text{Al}_2\text{O}_3$  surfaces and then major reduction and nitridation occurred beyond  $1300^\circ\text{C}$  (region VI).

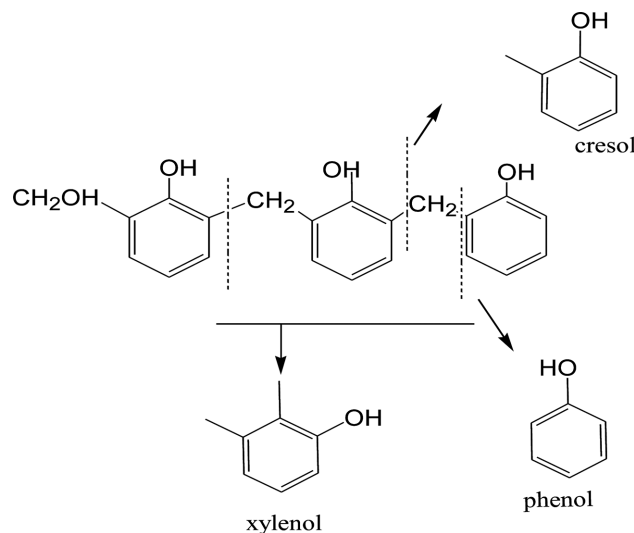


Fig. 1. Formation of phenols in the major weight-loss region

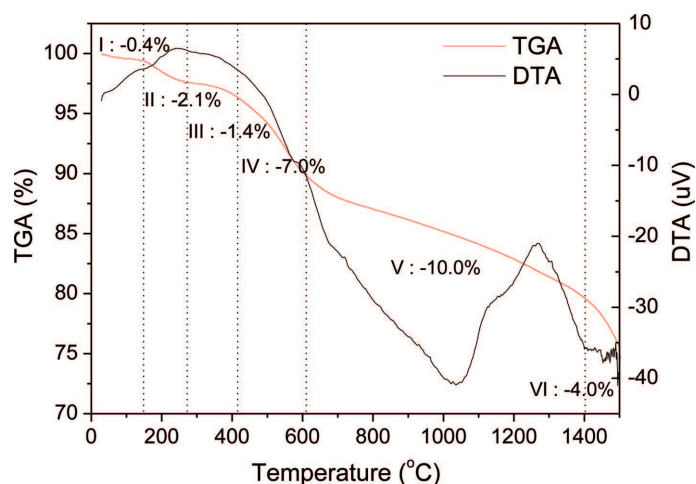
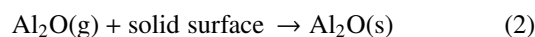
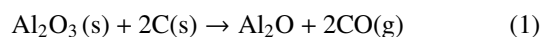


Fig. 2. DTA and TG analyses of  $\text{Al}_2\text{O}_3$ /phenol resin precursor

X-ray diffraction patterns of the precursor and the products that were synthesized in flowing nitrogen gas at various temperatures in the range of  $1300\text{--}1800^\circ\text{C}$  for 2h are shown in Fig. 3. It can be seen clearly that only  $\alpha\text{-Al}_2\text{O}_3$  phase peaks in the precursors can be detected, which indicates that the precursor consists of crystalline  $\alpha\text{-Al}_2\text{O}_3$  and amorphous carbon. Only  $\alpha\text{-Al}_2\text{O}_3$  phase can be detected in the sample synthesized at  $1300^\circ\text{C}$ . As also shown in Fig. 2, the weight loss of about 8.5% could be attributed to the carbothermal reduction reaction.



In the sample synthesized at  $1400^\circ\text{C}$ , weak diffraction peaks of hexagonal AlN (h-AlN) were detected together with the

diffraction peaks of  $\alpha$ -Al<sub>2</sub>O<sub>3</sub> and above 1400°C, the weight decreased rapidly, which indicates that the carbothermal nitridation reaction starts to occur at 1400°C and h-AlN were formed via the following reaction.

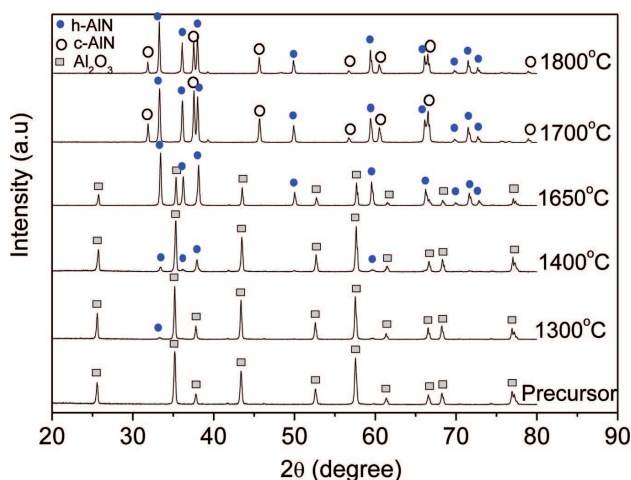
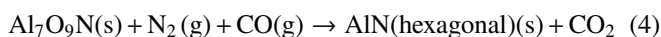
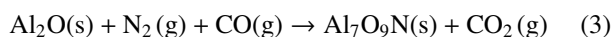
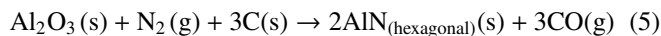


Fig. 3. XRD patterns of the precursor and the products synthesized at different temperatures



According to (1), (2), (3) and (4):



The intensities of former peaks increased as the temperature was increased from 1400°C to 1650°C, which showed that the crystallinity of AlN increases with temperature. In the sample was synthesized at 1650°C, the major crystal phase is h-AlN phase, while  $\alpha$ -Al<sub>2</sub>O<sub>3</sub> diffraction peaks also remain. At the ranges of 1700-1800°C, cubic AlN (c-AlN) phase appeared with h-AlN phase, and  $\alpha$ -Al<sub>2</sub>O<sub>3</sub> phase disappeared totally.  $\alpha$ -Al<sub>2</sub>O<sub>3</sub> completely converted to AlN. It is well accepted that the formation of AlON can occur at above 1650°C [18], which is an intermediate phase in carbothermal reduction. AlON formation is avoided even though the reaction goes above 1700°C, because AlON has the same cubic symmetry as cubic AlN. The nitrogen distribution in cubic AlN is cubic and closed packed, and non-metal arrangement in AlON into cubic AlN needs a slight adjustment in the cation positions and proportions in the carbothermal reduction reaction. Once AlON phase is formed in reaction, the excess carbon further reduces and AlON transforms into cubic AlN via further nitridation. Finally, hexagonal AlN phase is obtained via crystalline transition of unstable cubic AlN.

Figure 4 shows the effect of synthesis temperatures on the conversion ratios of  $\alpha$ -Al<sub>2</sub>O<sub>3</sub> to AlN, which are calculated on the basis of the AlN phase in XRD patterns. As shown in Fig. 4, nitridation reaction proceeds via three stages in temperature range of 1300-1800°C. Under 1300°C (stage I), there is Al<sub>2</sub>O<sub>3</sub> stable, which tells us that the temperature below 1300°C is not enough to reduce and nitride Al<sub>2</sub>O<sub>3</sub>. Compared with the aluminum oxide – carbon black system which usually requires a reactions temperature about 1800°C

for 5h for complete conversion [15], our reaction system had high reactivity, and lowered the temperature for the synthesis of AlN. It is generally accepted that the reaction rate is closely related to homogenous mixing of the raw materials. In our preparation of the precursor, carbon source exists as phenol resin liquid phase, and solid-gel precursors were homogeneously mixed. During the nitridation proceeds, alumina uniformly dispersed into the activated carbon matrix, which is formed by the dehydration and carbonization of phenol resin. The homogeneous mixing of alumina and carbon particles is thought as a reason for the high reactivity of our system and lowering the temperature of AlN formation. In the region I, Al<sub>2</sub>O<sub>3</sub> crystal phase only existed. At the range of 1400-1650°C (region II, carbothermal reduction stage), the amount of h-AlN increased rapidly and the quantity of  $\alpha$ -Al<sub>2</sub>O<sub>3</sub> decreased simultaneously. In the range of 1650-1700°C, c-AlN phase appeared and the amount of c-AlN decreased with temperature in the range of 1700 and 1800°C, which indicates that c-AlN phase exists as a metastable phase in the temperature region (region III, h-AlN and c-AlN cogeneration region). The ratio of h-AlN and c-AlN were 59% and 41% at 1700°C, respectively. Over 1700°C, it is thought that c-AlN phase transforms to h-AlN which is more stable crystal phase. Therefore, the quantity of c-AlN decreased to 31% at 1800°C.

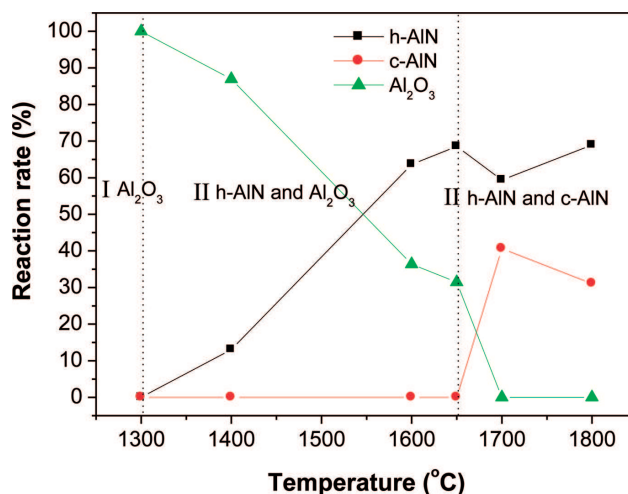


Fig. 4. Reaction rate (%) of Al<sub>2</sub>O<sub>3</sub> and formation rate (%) of h-AlN and c-AlN with different synthesis temperatures

Arrhenius equation gives “the dependence of the rate constant  $k$  of chemical reactions on the temperature  $T$  (in absolute temperature Kelvin) and activation energy  $E_a$ .”

$$k = A e^{-E_a/RT} \quad (6)$$

Where  $A$  is the pre-exponential constant,  $E_a$ , the activation energy for the reaction,  $R$ , the gas constant, and  $T$ , the absolute temperature.

Equation (6) could be expressed as:

$$\ln k = \ln A - \frac{E_a}{RT} \quad (7)$$

In Figure 5, the nitridation reaction constant  $k$  was calculated from Fig. 4. To determine the activation energy of h-AlN, c-AlN and AlN (both h-AlN and c-AlN) formation, natural logarithm reaction constant ( $\ln k$ ) is plotted against  $1/T$

and shown in Fig. 5 and Table 1. The activation energy ( $E_a$ ) for the formation of AlN was calculated from the slope of the graph ( $E_q$ . 7), which is about  $-206 \text{ kJ mol}^{-1}$  in the range  $1300\text{-}1650^\circ\text{C}$  (AlN obtain h-AlN phase), and  $-80 \text{ kJ mol}^{-1}$  between  $1700$  and  $1800^\circ\text{C}$  (AlN obtain h-AlN and c-AlN phase). However,  $E_a$  is  $-8 \text{ kJ mol}^{-1}$  for formation of h-AlN and  $91 \text{ kJ mol}^{-1}$  for formation of c-AlN in the range of  $1700\text{-}1800^\circ\text{C}$ , indicated that c-AlN is a metastable phase and the transformation of c-AlN to h-AlN continues with increasing the reaction temperature.

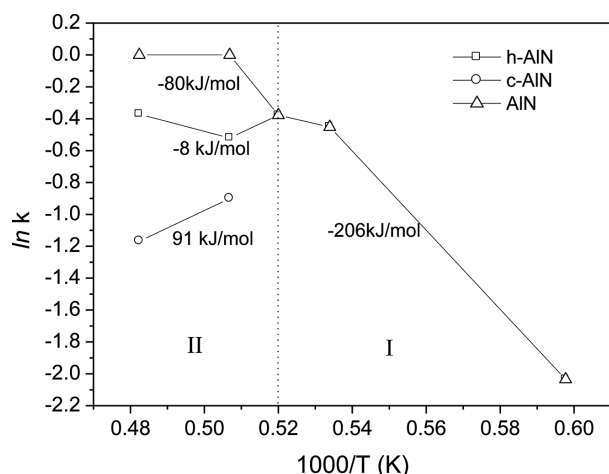


Fig. 5. Formation rate variations ( $\ln k$ ) of h-AlN, c-AlN, and AlN with ( $1000/T$ )

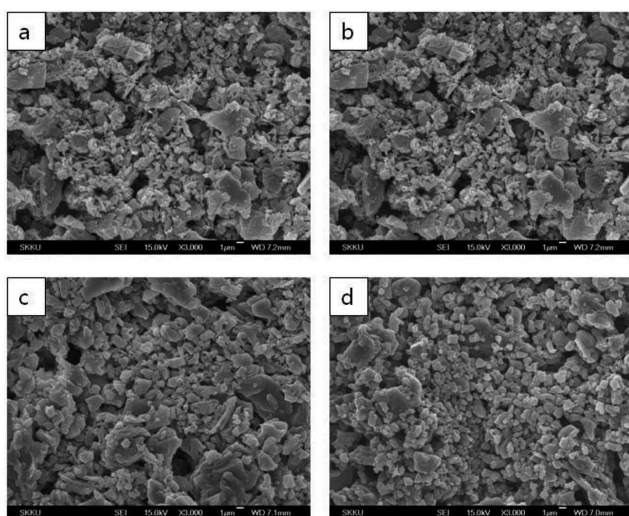


Fig. 6. FE-SEM photographs of the products synthesized at different temperatures (a)  $1600^\circ\text{C}$ ; (b)  $1650^\circ\text{C}$ ; (c)  $1700^\circ\text{C}$ ; (d)  $1800^\circ\text{C}$

Figure 6 shows FE-SEM images of the products synthesized at  $1600\text{-}1800^\circ\text{C}$ . The particles sizes are shown in Fig. 7. The particle size decreased with increasing temperatures from  $0.85$  to  $0.7 \mu\text{m}$ , probably due to the reduction of  $\alpha\text{-Al}_2\text{O}_3$ . The oxygen diffusion from inside to outside and nitridation of  $\text{Al}_2\text{O}_3$ , via nitrogen gas diffusion into inside, which cracked the original aluminum oxide crystals.

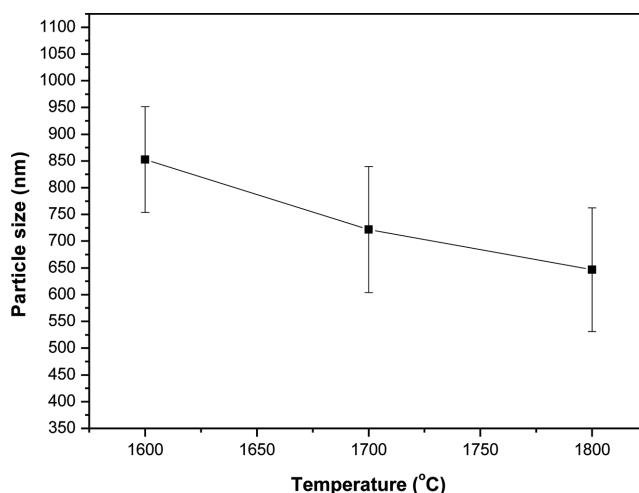


Fig. 7. Particles sizes of the products at the different temperatures

#### 4. Conclusions

Hexagonal and cubic crystalline aluminum nitride (AlN) particles were successfully synthesized using phenol resin and  $\alpha\text{-Al}_2\text{O}_3$  as precursors through new solid-gel mixing and carbothermal reduction nitridation process with molar ratio of  $\text{C}/\text{Al}_2\text{O}_3 = 3$ . The results showed that  $\alpha\text{-Al}_2\text{O}_3$  in homogeneous solid-gel precursor was easily nitrided to form AlN powder at relatively lower temperature. The reaction temperature needed for a complete conversion of  $\alpha\text{-Al}_2\text{O}_3$  to AlN was  $1700^\circ\text{C}$ , which much lower than that when using  $\alpha\text{-Al}_2\text{O}_3$  and carbon black as starting materials. We also found that h-AlN and c-AlN could be also produced between  $1700$  and  $1800^\circ\text{C}$ . However, c-AlN is considered to be a metastable crystal phase and disappear over  $1800^\circ\text{C}$ . There are three crystal phase regions;  $\text{Al}_2\text{O}_3$  stable region under  $1400^\circ\text{C}$  (region I), h-AlN formation and growth region between  $1400$  and  $1650^\circ\text{C}$  (region II), and complete formation of AlN (coexistence of

TABLE 1

Crystal phases (%), activation energies ( $E_a$ ), and crystal sizes with different reaction temperatures

Items		1300°C	1400°C	1600°C	1650°C	1700°C	1800°C
Temperature	Al <sub>2</sub> O <sub>3</sub>	100	87	36	31	0	0
	h-AlN	0	13	64	69	58	64
	c-AlN	0	0	0	0	42	36
$E_a$ kJ/mol	AlN	-206				-80	
	h-AlN					-8	
	c-AlN					91	
Crystal size (um)		-			0.85	0.75	0.7



h-AlN and c-AlN; region III). In the region II, the activation energy is large, -206kJ/mol, and small -80kJ/mol in the region III, where c-AlN has 91kJ/mol as a metastable phase. Phenol resin is a useful carbon source for AlN synthesis via CRN process, which is an efficient, economical, cheap reagent for large-scale synthesis of AlN powder.

#### Acknowledgements

This research was supported by the program of Industrial Convergence Resources Research Program (grant no. 10038631) of the Ministry of Knowledge and Economy (MKE).

#### REFERENCES

- [1] B.H. Mussler, J. Am. Ceram. Soc. Bull **79**, 45-47 (2000).
- [2] L.M. Sheppard, J. Am. Ceram. Soc. Bull **69**, 1801-1812 (1990).
- [3] L.C. Pathak, A.K. Ray, S. Das, C.S. Sivaramakrishnan, P. Ramachandrarao, J. Am. Ceram. Soc. **82** [1], 257-260 (1999).
- [4] M.L. Qin, X.L. Du, J. Wang, I.S. Humail, X.H. Qu, J. Eur. Ceram. Soc. **29** [4], 795-799 (2009).
- [5] T. Yamakawa, J. Tatami, T. Wakihara, K. Komeya, T. Meguro, K.J.D. MacKenzie, S. Takagi, M. Yokouchi, J. Am. Ceram. Soc. **89** [5], 171-175 (2006).
- [6] A.A. Adjaottor, G.L. Griffin, J. Am. Ceram. Soc. **75** [12], 3209-3214 (1992).
- [7] M.L. Panchula, J.Y. Ying, J. Am. Ceram. Soc. **86** [7], 1114-1120 (2003).
- [8] M. Iwata, K. Adachi, S. Furukawa, T. Amakawa, J. Phys. D: Appl. Phys. **37** [7], 1041-1047 (2004).
- [9] K. Baba, N. Shohata, M. Yonezawa, J. Appl. Phys. Lett. **54** [23], 2309-2311 (1989).
- [10] R. Fu, K. Chen, S. Agathopoulos, J.M.F. Ferreira, J. Cryst. Growth **296** [1], 97-103 (2006).
- [11] H.B. Wang, J.C. Han, Z.Q. Li, S.Y. Du, J. Eur. Ceram. Soc. **21** [12], 2193-2198 (2001).
- [12] G. Selvaduray, L. Sheet, J. Mater. Sci. Technol. **9** [6], 463-73 (1993).
- [13] L.D. Silverman, J. Adv. Ceram. Mater **3** [4], 418-419 (1988).
- [14] N. Hashimoto, H. Yoden, K. Nomura, J. Am. Ceram. Soc. **74** [6], 1282-1286 (1991).
- [15] J. Wang, W.L. Wang, P.D. Ding, J. Diamond. Relat. Mater. **8**[7], 1342-1344 (1999).
- [16] Y.K. Lee, D.J. Kim, H.J. Kim, T.S. Hwang, M. Rafailovich, J. Sokolov, J. of App. Polym. Sci. **89**, 2589-2597 (2003).
- [17] J.-M. Lin, C.-C. Ma, M. Polym. Degrad. Stab. **69**, 229 (2000).
- [18] J.C. Kuang, C.R. Zhang, X.G. Zhou, Q.C. Liu, C. Ye, J. Mater. Lett. **59**[16], 2006-2010 (2005).